Improved Therapeutic Effectiveness by Combining Recombinant CXC Chemokine Ligand 10 with Cisplatin in Solid Tumors

Gang Li,[1,2] LingTian,[1] Jian-mei Hou,[1] Zhen-yu Ding,[1] Qiu-ming He,[1] Ping Feng,[1] Yan-jun Wen,[1] Fei Xiao,[1] Bing Yao,[1] Ru Zhang,[1] Feng Peng,[1] Yu Jiang,[1] Feng Luo,[1] Xia Zhao,[1] Lin Zhang,[1] Qiao Zhou,[1] and Yu-quan Wei[1]

Abstract

Purpose: CXC chemokine ligand 10 (CXCL10) is a potent inhibitor of angiogenesis. We wonder whether the combination of CXCL10 with cisplatin would improve the therapeutic antitumor efficacy.

Experiment Design: We evaluated the antitumor activity of the combination therapy in the immunocompetent C57BL/6 and BALB/c mice bearing LL/2 Lewis lung cancer and CT26 colon adenocarcinoma , respectively. Mice were treated with either CXCL10 s.c. at 25 μg per kg per day once daily for 30 days, cisplatin cycled twice (5 mg/kg i.p. on days 14 and 21 after the initiation of CXCL10), or both agents together. Tumor volume and survival time were observed. Antiangiogenesis of CXCL10 *in vivo* were determined by alginate capsule models and CD31 immunohistochemistry. Histologic analysis and assessment of apoptotic cells were also conducted in tumor tissues.

Results: CXCL10 + cisplatin reduced tumor growth in LL/2 and CT26 tumor model, respectively, more effectively, although cisplatin or CXCL10 individually resulted in suppression of tumor growth and improved survival time of tumor-bearing mice. CXCL10 successfully inhibited angiogenesis as assessed by alginate model and CD31 ($P < 0.05$). Histologic analysis of tumors exhibited that CXCL10 in combination with cisplatin led to the increased rate of apoptosis, tumor necrosis, and elevated lymphocyte infiltration.

Conclusions: Our data suggest that the combination of CXCL10, a well-tolerated angiogenesis inhibitor, with cisplatin can enhance the antitumor activity. The present findings may be of importance to the further exploration of the potential application of this combined approach in the treatment of lung and colon carcinoma.

Cytotoxic chemotherapy has been the mainstay of medical approaches to the treatment of solid cancers. Cisplatin (DDP) remains the most widely used first-line element of cytotoxic chemotherapy to solid tumors (1). However, the efficacy of DDP based on the treatment is limited in curing most solid tumors due to dose-dependent toxicity. Therefore, several new therapeutic strategies under investigation involve modulation of cellular chemosensitivity, including the inhibition of tumor neovascularization, reversing tumor resistance, and increasing therapeutic effects of chemotherapy (2, 3). Angiogenesis inhibitors are likely to be relatively noncytotoxic, to exhibit a different spectrum of deleterious effects than those caused by the toxic agents (4, 5), and to work well in combination with chemotherapy (6–11).

To date, many agents including CXC chemokine have been identified as angiogenesis inhibitors. The CXC chemokines are a unique family of cytokines for their ability to behave in a disparate manner in the regulation of angiogenesis (12–17). A second structural domain within this family determines their angiogenic potential. Members that contain the three amino acids (Glu-Leu-Arg)/ELR immediately NH_2-terminal to the CXC motif (ELR^+) are potent promoters of angiogenesis and stimulate the endothelial cell chemotaxis (e.g., interleukin-8). In contrast, the members that are induced by IFN and lack the ELR motif (ELR^-) are potent inhibitors of angiogenesis, such as platelet factor-4 (PF4), monokine induced by IFN-γ (MIG, CXCL9), IFN-inducible T cell α chemoattractant (I-TAC, CXCL11), and CXC chemokine ligand 10 (CXCL10, IP-10).

CXCL10 is a potent inhibitor of angiogenesis and displays some thymus-dependent antitumor effect (16, 18–21). Therapy with CXCL10 is effective in reducing the rate of tumor growth, whereas it fails to induce tumor complete regression (21–24), which suggests that further treatment may require supplemental drugs targeting directly the tumor cells.

Authors' Affiliations: [1]State Key Laboratory of Biotherapy and Cancer Center, West China Hospital, West China Medical School, Sichuan University, Chengdu, Sichuan, The People's Republic of China; and [2]Cancer Center, Three Gorges Central Hospital of Chongqing, Chongqing, The People's Republic of China

Received 10/17/04; revised 2/8/05; accepted 2/25/05.

Grant support: National Basic Research Program of China grants 2001CB510001 and 2004CB51880, National Natural Science Foundation of China projects, National 863 Program, and CMB.

The costs of publication of this article were defrayed in part by the payment of page charges. This article must therefore be hereby marked *advertisement* in accordance with 18 U.S.C. Section 1734 solely to indicate this fact.

Note: G. Li and L. Tian contributed equally to this work.

Requests for reprints: Yu-quan Wei, State Key Laboratory of Biotherapy and Cancer Center, West China Hospital, West China Medical School, Sichuan University, Guo Xue Xiang No. 37, Chengdu, Sichuan, 610041, The People's Republic of China. Fax: 86-28-85250731; E-mail: yuquawei@vip.sina.com or yuquawei@hotmail.com.

Moreover, the recent findings from other groups indicated that to successfully counteract tumor progression, drugs inhibiting new vasculature formation should be employed in combination with traditional antitumor strategies, such as chemotherapy or radiotherapy (6–11, 25).

It has been shown that some CXC chemokines supported the survival of normal hematopoietic cells but not cancer cells and acted as chemoprotectant (26). Sarris et al. had also speculated that CXCL10 might be exploited to protect hematopoietic progenitors from the cytotoxic effects of chemotherapy (27). DDP-based chemotherapy often accompanied dose-limiting toxicity including bone marrow suppression. One approach is to maintain stem cells in a quiescent state during the periods of chemotherapy so that the cells have an increased period during which the repair of lethal damage may proceed before replication. For instance, evidence had indicated that normal hematopoietic cells treated by PF4 are still viable but at a relatively quiescent state. Thus, they are less sensitive to damage caused by cytotoxic drugs (26). Thus, we wonder whether it would improve the therapeutic efficacy of the antitumor by combining DDP with CXCL10. The present article showed that cooperated administration of DDP with CXCL10 improved therapeutic effectiveness in tumor-bearing immunocompetent animals.

Materials and Methods

Preparation of recombinant CXCL10. The nucleotide sequence encoding the mature region of murine CXCL10 cDNA (Genbank accession no. m33266; ref. 15) was PCR amplified from pBLAST-mIP-10 (Invivogen) and cloned into an expression plasmid pET-32a (Novagen). Recombinant mCXCL10 protein was generated in *Escherichia coli*. It was renatured by dropwise addition to 20 mmol/L phosphate buffer (pH 8.5) containing 0.1 mmol/L oxidized glutathione and 1 mmol/L reduced glutathione at 4°C. Purified mCXCL10 was prepared using a nickel-chelating column (Chelating Sepharose Fast Flow, Amersham Pharmacia Biotech, Uppsala, Sweden) on the chromatography system (AKTA, Amersham Pharmacia Biotech). The protein was eluted from the column with a linear gradient of imidazole, which was then dialyzed against the buffer containing decreased imidazole concentration. Finally, it was dialyzed by PBS. Recombinant proteins were further purified by ion exchange and gel filtration chromatography. The fusion protein has an enterokinase cleavage site between thioredoxin protein and CXCL10. Thioredoxin protein was cleaved from the fusion protein by enterokinase (Novagen). Fractions containing pure CXCL10 were identified by Tricine-PAGE and Western blot analysis as described previously (28). Membrane blots were probed with rabbit anti-murine CXCL10 antibody from Peprotech (Rocky Hill, NJ). Goat anti-rabbit immunoglobulin G linked to alkaline phosphatase (Sigma, St. Louis, MO), 5-bromo-4-chloro-3-indoyl phosphate *p*-toluidine salt, and *p*-nitroblue tetrazolium chloride color substrate (Bio-Rad, Richmond, CA) was used for detection. Protein concentration was determined by the Bradford assay using the Bio-Rad Protein Assay reagent (Bio-Rad) with bovine serum albumin (Sigma) as a standard. All protein preparation used in animal studies were filter sterilized, also tested for endotoxin, separated into aliquots, and frozen at −20°C.

***Chemotaxis assay* in vitro.** Biological activity was evaluated by chemotaxis as previously described (29) with slight modification. T lymphocytes separated from mouse spleen stimulated for 2 days with 1 μg/mL phytohemagglutinin (Murex Diagnosis, Dartford, United Kingdom) and 400 units/mL interleukin-2 (Sigma) in RPMI 1640. Chemokine dilution medium supplemented with 1% low endotoxin bovine serum albumin was added to the bottom well of a 96-well Boyden microchambers chemotaxis plate (Neuroprobe). Fifty microliters of lymphocyte cells at the concentration of 5×10^6 cells/mL were added on top of the membrane (5 μm pore size, polycarbonate filters, polyvinylpyrrolidone-free polycarbonate membranes). The chemotaxis plate was incubated at 37°C in an atmosphere containing 5% CO_2 for 4 hours and transferred to 4°C for 10 minutes before removing the membrane, fixed in 70% methanol, and stained for 5 minutes in 1% Coomassie brilliant blue. The number of cells that migrated to the lower surface was microscopically counted at six randomly chosen high power fields. Commercially available murine IFN-γ inducible protein 10 (IP-10) from Peprotech with biological activity was used as standard control. For the blocking experiments, bottom chamber was added with 30 μg/mL of rabbit anti-mCXCL10 antibody from Peprotech or control rabbit immunoglobulin G (Sigma). Three replicates were done for each treatment.

Tumor model. All studies involving mice were approved by the institute's Animal Care and Use Committee. CT26 colon adenocarcinoma and LL/2 Lewis lung cancer models were established in immunocompetent BALB/c and C57BL/6 mice at 6 to 8 weeks of age, respectively, as previously described (30).

Tumor growth inhibition study. Mice were weighed, coded, and divided into different groups when tumor was ~90 mm^3 after tumor cell inoculation. The experiment for the observation of tumor volume and survival advantage included 10 mice per group. Mice bearing established tumors were given systemically s.c. with mCXCL10 at 25 μg per kg per day, an effective dosage previously reported (20), once a day for 30 days in a volume of 0.1 mL at left flank, or appropriate controls injection in a volume of 0.1 mL PBS solution at the same time point. The regime of DDP (Qilu Pharmaceutical Co., Shandong, China) was cycled twice (5 mg/kg i.p. on days 14 and 21 after the initiation of CXCL10 administration) in 0.1 mL saline. Survival time and tumor volume were observed. Tumor size was determined by caliper measurement of the largest and perpendicular diameters every 4 days. Tumor volume was calculated according to the formula $V = 0.52ab^2$, where a is the largest superficial diameter and b is the smallest superficial diameter. The mice were sacrificed when they became moribund.

To evaluate the tumor weight and immunohistochemistry, the mice were killed by cervical dislocation on day 4 after the completion of treatment as described above. Excised tumors were weighed before their fixation in 10% formalin. In these models, the [mean excised treated-tumor weight divided by the mean excised control-tumor weight] × 100% was subtracted from 100% to give the tumor growth inhibition value for each group.

Alginate-encapsulated tumor cells assay. An alginate-encapsulated assay was done *in vivo* as previously described (31, 32). CT26 colon adenocarcinoma cells were resuspended in a 1.5% solution of sodium alginate (Sigma) and were added dropwise into a solution of 250 mmol/L calcium chloride. Alginate beads containing 1×10^5 tumor cells per bead were formed. Four beads were then implanted s.c. into an incision made on the dorsal side of the BALB/c mice. Mice were subdivided into four groups and treated with PBS, CXCL10 alone, DDP alone, or CXCL10 + DDP (five mice per group), respectively. Treatment was initiated on day 2 with CXCL10 s.c. at 25 μg per kg per day continually for 14 days and/or DDP 5 mg/kg i.p. on days 4 and 10 after alginate beads grafting. Additional control animals were injected with PBS as described above. On day 15 after implanting, the mice were injected i.v. with 0.1 mL of a 100 mg/kg FITC-dextran (Sigma) solution through the tail vein. Alginate beads were rapidly removed and photographed 20 minutes after FITC-dextran introduction. The uptake of FITC-dextran was measured against a standard curve of FITC-dextran.

Histologic analysis. Sections of paraffin embedded from each group were stained with H&E. H&E section along the largest diameter of the tumor was scanned in the low field using the computer aided image analysis system Quantimet 600 and Qwin software (Leica, Benshaim, Germany). The total tumor area and necrotic tumor area were subsequently marked by the examiners on the screen. The areas were

evaluated by the image analysis system, and the ratio tumor necrosis area to total tumor area was given in percentages. Leukocytes were quantitated as previously described (21). The organs such as lungs, liver, kidneys, etc. were also isolated for histology.

CXCL10-induced antiangiogenesis was determined by immunohistologic analysis of neovascularization in tumors. Tumors were embedded in paraffin, sectioned at 4 μm, deparaffinized in xylenes, and rehydrated through the graded ethanol into PBS. Antigen retrieval was done by microwaving in 10 mmol/L EDTA (pH 6.0); incubated with rat anti-mouse CD31 (platelet/endothelial cell adhesion molecule 1) polyclonal antibody (1:50; PharMingen, San Diego, CA), at 4°C, washed, incubated with biotinylated secondary antibody at room temperature for 30 minutes, washed, and incubated with avidin–biotin–horseradish peroxidase complex (Vectastain Elite; Vector Laboratories, Burlingame, CA), according to the manufacturer's instructions. Quantification was done as described by Vermeulen et al. (33). Microvessel counting was done at ×200. The results regarding angiogenesis were expressed as the absolute number of the microvessel per high-power field of three sections in each tumor.

Quantitative assessment of apoptosis. Tumor species were prepared as described above. Terminal deoxynucleotidyl transferase–mediated nick-end labeling staining was done using an *in situ* cell death detection kit (Roche Molecular Biochemicals) following the manufacturer's protocol. It is based on the enzymatic addition of digoxigenin nucleotide to the nicked DNA by terminal deoxynucleotidyl transferase. In tissue sections, four equal-sized fields were randomly chosen and analyzed. Density was evaluated in each field, yielding the density of apoptotic cells (apoptosis index).

Observation of potential toxicity. The toxicities of the treatment regimens were estimated by changes in animal body weight and the incidence of drug-associated death. Blood were obtained from the tail vein for complete blood count and enzyme analysis. Possible side effects of protein had been studied as previously described (30). The mice treated with recombinant CXCL10 s.c. without carcinomatosis have been investigated, in particular for potential toxicity, for >4 months. Gross measures, such as weight loss, ruffling of fur, life span, behavior, and feeding were studied. Tissues of heart, liver, spleen, lung, kidney, brain, bone marrow, etc. were also fixed in 10% neutral buffered formalin solution and embedded in paraffin. Sections of 4 μm were stained with H&E. Possible autoreactive antibody in serum of mice at various time points was determined by ELISA.

The combination of cytokines with chemotherapy may not be entirely innocuous because they may exacerbate an already present marrow reconstitutive defect such as residual cytopenias and marrow hypoplasia. Therefore, animals were subjected to complete peripheral blood counts and differentials. Evaluation of effects on hematopoiesis was conducted similar to previously described (34). Normal BALB/c and C57BL/6 mice (n = 5 per group) were given systemically s.c. with mCXCL10 at 10 or 25 μg per kg per day once daily for 30 days. The control group was injected with 0.1 mL PBS solution containing 1% bovine serum albumin. The mice were sacrificed on day 4 after terminating treatment. The tibiofibula were exposed by dissection and removed by cutting the bone as near to the malleolus and condyle as possible. The bone marrow was obtained by inserting a 23-gauge needle into the condyle end of the bone, and the cells were flushed out with 1 mL of PBS containing 1 unit/mL heparin. The leukocytes, erythrocytes, and platelets were enumerated. Cell cycle distribution was assessed as described by Vindelov et al. (35). Cells were processed and stained with propidium iodide, analyzed by flow cytometry (ESP Elite, Coulter). Cell cycle analysis was done using the sum of broadened rectangles model with the DNA software from Becton Dickinson (Mountain View, CA).

Statistical analysis. Data was assayed by ANOVA and Student's t test. For the survival time of animals, Kaplan-Meier curves were established for each group, and the survivals were compared by means of the log-rank test. Differences between means or ranks as appropriate were considered significant when yielding a $P < 0.05$.

Results

Determination of biologically active CXCL10. Murine CXCL10 was expressed in *E. coli* as a fusion protein. Nickel chelataffinity chromatography was employed to purify large quantities of mCXCL10. Enterokinase was used to cleave the CXCL10 fusion protein. CXCL10 after purification and cleaviation has a predicted molecular mass of ~9.5 kDa. Purity was >95% as determined by Tricine-PAGE (Fig. 1A). It was further verified by Western blot (Fig. 1B). Physiologic properties mimicking native CXCL10 was determined by its chemoattraction ability. Commercially available recombinant murine IP-10 from Peprotech was used as standard control. Recombinant CXCL10 in our experiment has a similar capacity of chemotaxis compared with purchased IP-10 *in vitro*. Chemotactic index was declined when anti-CXCL10 was given. Chemotaxis assay indicated that refolding of CXCL10 resulted in product with complete biological activity for further animal experiment (Fig. 1C).

Tumor growth inhibition. Tumor volume and life span of mice assay showed that both CXCL10 and DDP individually

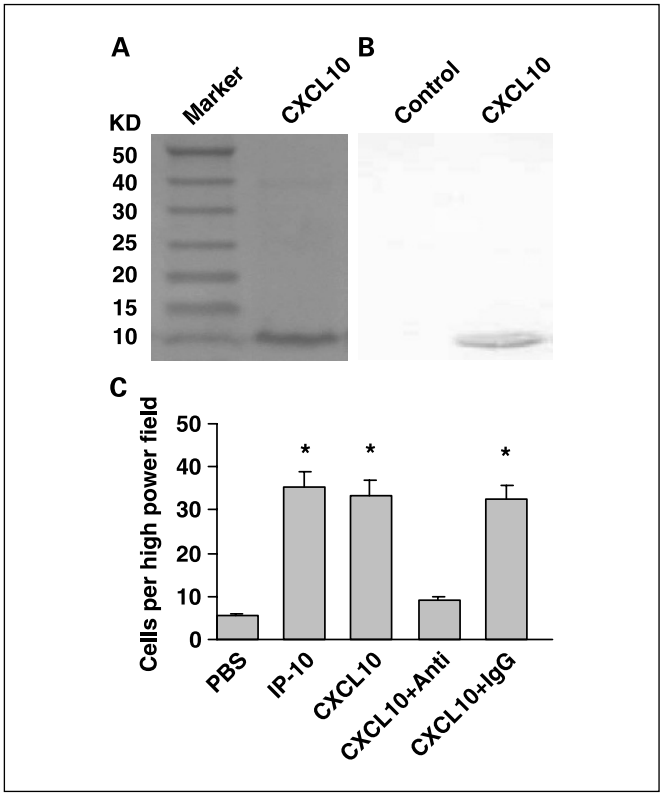

Fig. 1. Determination of biologically active CXCL10. Recombinant mCXCL10 was purified using a nickel-chelating column and assayed by Tricine-PAGE. The protein CXCL10 was further verified using Western blot. Chemotaxis activity was demonstrated with the addition of 50 ng/mL recombinant mCXCL10, or commercially available IP-10 as standard control. Neutralization was done by the pretreatment with the anti-mCXL10 antibody (30 μg/mL) or immunoglobulin G. Procedure for cell staining was described in Materials and Methods. The number of cells that migrated to the lower surface was microscopically counted at six randomly chosen high-power fields. *A*, Tricine-PAGE assay of purified recombinant murine CXCL10. *B*, Western blot analysis of recombinant mCXCL10. *C*, chemotactic assay of recombinant mCXCL10. Recombinant CXCL10 has similar capacity of chemotaxis compared with commercial IP-10 *in vitro*. Migrating cells was declined when anti-CXCL10 was administered. *, $P < 0.01$, significant chemotaxis differences relative to PBS control group. Three replicates were done for each treatment.

resulted in effective suppression of tumor growth. Combined treatment had a superior antitumor effect, resulting in 12- and 15-day (DDP 3.0 and 4.5 days) delay of tumor growth to reach a volume of 800 mm^3 compared with PBS control in CT26 and LL/2 (Fig. 2A). In the two tumor models, control animals that received PBS treatment survived 32.1 and 32.7 days on average, respectively. In contrast, the combination of CXCL10 therapy with DDP resulted in a significant 3-fold increase in life span ($P < 0.01$, by log-rank test; Fig. 2B). Systemic therapy with CXCL10 + DDP resulted in apparent tumor inhibition versus PBS controls ($P < 0.01$) and DDP or CXCL10 alone ($P < 0.05$). The tumor growth inhibition was calculated using the mean excised tumor weight after completion of treatment for each group. Additionally, the appearance of lung metastases was significantly delayed by treatment with CXCL10 or CXCL10 + DDP in comparison with PBS control.

Alginate encapsulation assay. The inhibition of angiogenesis was confirmed in the alginate-encapsulated tumor cell assay. Figure 3A-D shows representative images of tumor vasculature in CT26 colon adenocarcinoma–encapsuled alginate. The vascular plexus of the tumor in PBS group formed a ladder-like pattern, which was richly morphologic and irregular (Fig. 3A). The treated tumor exhibited relatively little vascularity (Fig. 3B-D). Vascularization of beads over 15 days can then be measured by uptake of FITC-dextran into beads. Vascularization of alginate beads was apparently reduced, and FITC-dextran uptake was decreased 83% in CXCL10-treated mice compared with that in PBS controls ($P < 0.05$). No significant difference was observed between DDP group and PBS control mice ($P = 0.17$; Fig. 3E).

Immunolabeling of CD31. We further quantified vessel density as measures of angiogenesis by immunolabeling of CD31 in tissue sections. The most highly vascularized area of each tumor was identified on low power and five high-powered fields were counted in this area of greatest vessel density. The combination of CXCL10 and DDP apparently reduced the number of vessels compared with control groups, including PBS or DDP alone ($P < 0.05$). Angiogenesis was also inhibited in the treatment with CXCL10 alone compared with controls. No statistically significant differences were obtained between DDP and PBS group ($P = 0.16$ and 0.25 in LL/2 and CT26, respectively; Fig. 4).

Therapeutic effect on apoptosis. To explore the role of CXCL10 on apoptosis of tumor cells, tumors resected 4 days after the completion of treatment were subjected to terminal deoxynucleotidyl transferase–mediated nick-end labeling assays for the respective determination of apoptotic index. DDP or CXCL10 alone treatment affected the apoptosis rate of tumor cells, whereas the density of apoptotic cancer cells increased after the combined therapy (Fig. 5A). Data represent the mean apoptotic index ± SDs of cancer cells as percent normalized to apoptotic index of cancer cells (Fig. 5B).

Histologic analysis. Histologically, those CXCL10-treated tumors showed visible responses with homogeneous necrosis that was distinguishable in size and morphology from the several focal necroses of DDP-responsive tumors. Control tumors displayed little or no tumor tissue necrosis and had normal capillaries surrounding nests of confluent tumor cells. Analysis of the extent of tumor necrosis revealed that the coadministration of the two agents was clearly more effective,

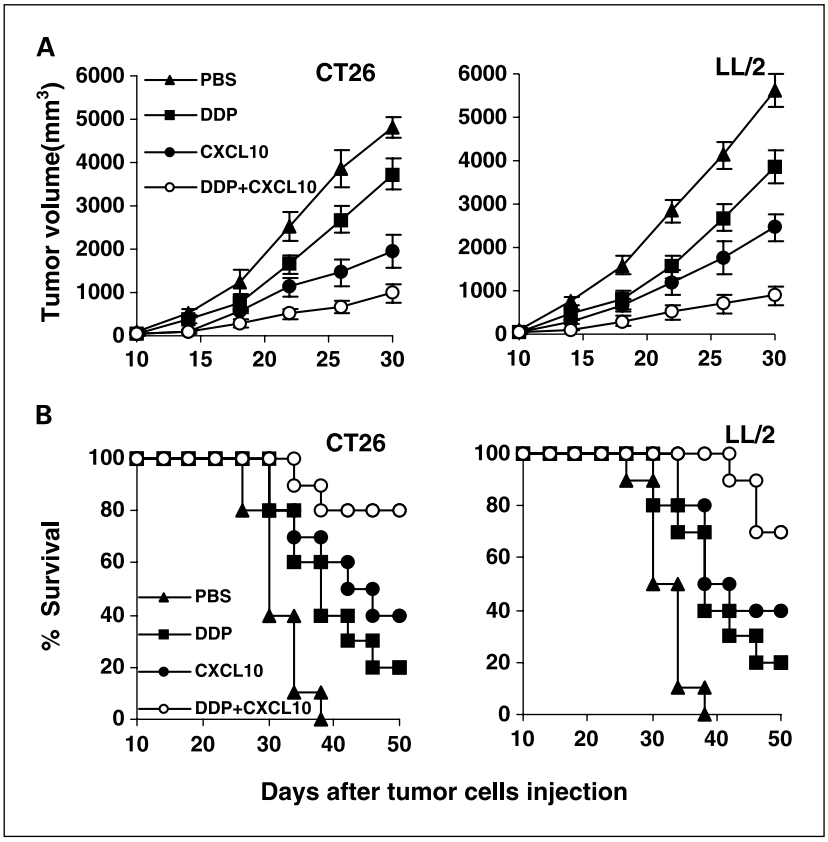

Fig. 2. Tumor suppression and survival advantage in mice. Mice (10 mice per group) were treated with injection of CXCL10 s.c. at 25 μg per kg per day once daily for 30 days and/or administration of DDP i.p. cycled twice (5 mg/kg, on days 14 and 21 after initiation of CXCL10) or appropriate controls 0.1 mL PBS at the same time point. Disease progression and outcome were determined as described in Materials and Methods. *A*, suppression of s.c. tumor growth in mice. Graph of systemic therapy with CXCL10 + DDP resulting in significant tumor growth inhibition versus PBS controls ($P < 0.01$), CXCL10 alone ($P < 0.05$) from day 20 after initiation of CXCL10 administration. Points, average tumor volume; bars, ±SD. *B*, a significant increase in survival in combined treatment mice compared with the control ($P < 0.01$, by log-rank test) was found in CT26. Similar result was also found in LL/2 tumor model.

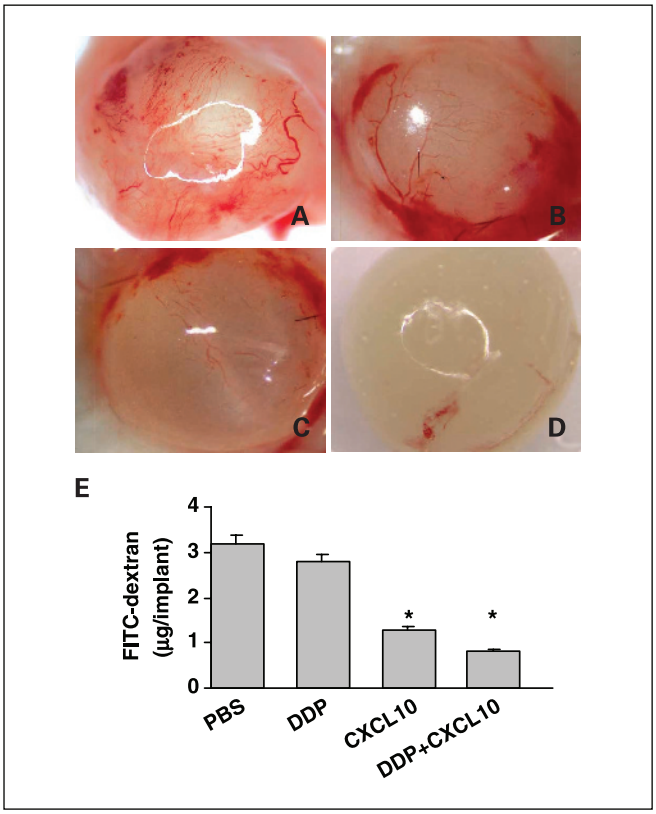

Fig. 3. Antiangiogenesis assay by alginate bead *in vivo*. Alginate beads containing 1×10^5 tumor cells were implanted s.c. into the backs of BALB/c mice (four beads per mice). Mice (five mice per group) treated with CXCL10 s.c. at 25 μg per kg per day continuously for 14 days, DDP i.p. cycled twice (5 mg/kg, on days 4 and 10 after initiation of CXCL10 administration), or both agents together after implanting. On day 15 after inoculation, beads were surgically removed. FITC-dextran was quantified as described in Materials and Methods. Representative images of alginate beads of PBS (*A*), DDP (*B*), CXCL10 (*C*), CXCL10 + DDP (*D*) under dissecting microscope (×10) and FITC-dextran quantification of alginate beads (*E*). Photograph of alginate implants and FITC-dextran uptake showed the reduction of vascularization in combination treatment group or CXCL10 alone – treated mice compared with PBS controls. *Columns*, means of 20 beads per group; *bars*, ±SD. *, $P < 0.05$ compared with PBS control.

eliciting a 2.5-fold increase in tumor necrosis relative to single-element treatment (Fig. 6A-D). Leukocyte infiltration was next evaluated by histology within the tumor tissue. Leukocyte infiltration exhibiting clustering-like aggregation was apparently found in the margin of both CXCL10 alone and CXCL10 in conjunction with DDP group. Representative sections of PBS control and CXCL10 treated from CT26 neoplasm tissue were depicted (Fig. 6E-F). Lymphocyte infiltration was also remarkably elevated in central regions from CXCL10- or CXCL10 + DDP – treated groups. Representative sections of PBS control and CXCL10 treated from CT26 neoplasm tissue were depicted (Fig. 6G-H). Quantitation of tumor-infiltrating leukocytes revealed apparent difference in CXCL10 or CXCL10 + DDP relative to PBS treated (both $P < 0.01$).

Observation of potential toxicity. The systemic administration of cytokines can elicit antitumor effects, but the toxicities associated with this treatment occasionally resembled a state of severe infection and therefore can be limited (36, 37). Thus, CXCL10-treated animals without tumor burden were particularly investigated for potential toxicity of CXCL10 for >4 months. None of pathologic changes in liver, lung, kidney, etc. were found by microscopic examination after administration of CXCL10. No adverse consequences were showed in gross measures, such as weight loss, ruffling of fur, life span, behavior, or feeding. No autoreactive antibody in serum can be determined by ELISA. For evaluation of the effects of CXCL10 on hematopoiesis, animals were subjected to complete peripheral blood counts and differentials. Analysis of peripheral blood revealed that no significant difference was observed between DDP-treated and the combined treatment group. Our data suggested that traditional chemotherapeutic DDP in combination with CXCL10 was concurrently practicable with less host toxicity. In addition, bone marrow cells were enumerated and analyzed by microscope and cell cycles were analyzed by flow cytometry. No decreased or compensating hematopoiesis was found. There was also no apparent difference in the percent of G_0-G_1 or S-phase cell distribution between PBS-treated and CXCL10-treated (10 μg per kg per day) and CXCL10-treated (25 μg per kg per day) group (both $P > 0.05$, $n = 5$) in CT26 tumor. Neither accumulation of hematopoietic stem cells in the G_0 phase nor reduction in the percentage of cells in the S phase was observed. Similar results were also found in LL/2 neoplasm model (data not shown).

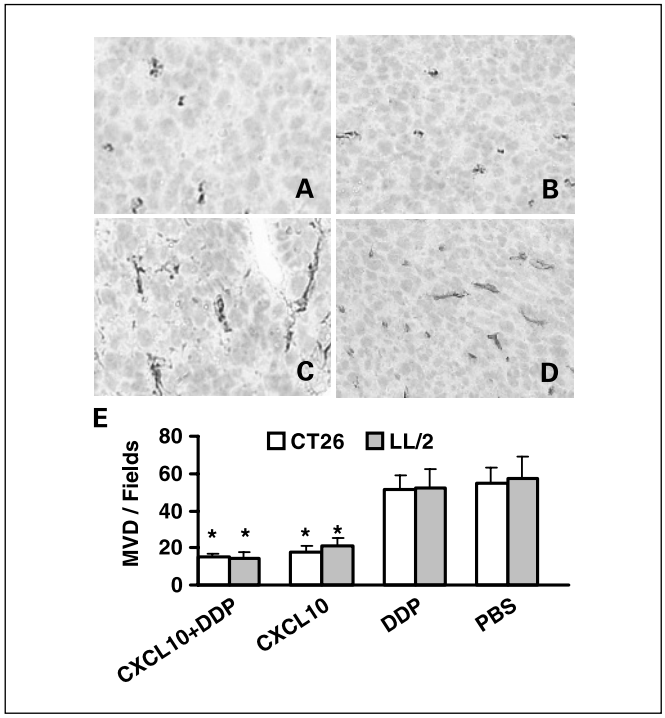

Fig. 4. Inhibition of angiogenesis assayed by immunohistochemistry with CD31. Mice bearing established tumors were administered systemically s.c. with mCXCL10 at 25 μg per kg per day once daily for 30 days, and/or DDP i.p. cycled twice (5 mg/kg, on days 14 and 21) or 0.1 mL PBS. Tumor angiogenesis was assessed by immunohistochemical staining with anti-CD31 antibody (*brown*) on paraffin-embedded sections of tumors resected 4 days after completion of treatment. Microvessel counting was done at ×200. DDP + CXCL10 – treated tumor revealed only occasional, isolated microvessels (*A*). The injection of CXCL10 alone (*B*) also has an angiostatic effect. At the same magnification, the section of representative images with well-formed capillaries surrounding nests of tumor cells in DDP (*C*) and PBS control treated (*D*). Combination treatment group displayed decreased microvessel as compared with PBS control in CT26 (*open columns*) and LL/2 (*closed columns*) tumor tissues in sequential analysis (*E*). *Columns*, mean of microvessel per high-power field; *bars*, ±SD. *, $P < 0.05$ relative to PBS control.

Discussion

The generation of new blood vessels, angiogenesis, is a complex multistep process, which is tightly regulated by many positive and negative factors (2). Angiogenesis is important for normal embryonic development and for the development of pathologic conditions, such as cancer, rheumatoid arthritis, retinopathies, etc. (3). Several lines of direct and indirect evidence indicate that the growth and persistence of solid tumors and their metastasis are angiogenesis dependent (4). As a strategy for cancer therapy, antiangiogenic therapy attempts to stop new vessels from forming around a tumor and break up the existing network of abnormal capillaries that feeds the cancerous mass (4). A number of new angiogenesis inhibitors are currently being explored in a series of clinical trials and unfolded an inspiring perspective (38). Antiangiogenic therapy, although effective in inhibiting tumor growth, has not been shown tumoricidal in most studies (39). This therapeutic limitation can be overcome by combining angiogenesis inhibitors with cytotoxic therapies (6–11). CXCL10 as a potent angiostatic protein alone has also been used in antineoplasm in the tumor model in mice (20–23). The present study was designed to determine whether cisplatin potentiates the antitumor activity of CXCL10. The data in the present study showed that the combined treatment with CXCL10 and DDP led to an enhanced antitumor growth and the increased induction of apoptosis compared with CXCL10 and DDP alone. To our knowledge, this is the first time that CXCL10 and chemotherapy have been tested together and found to have the enhanced inhibitory effects on colon and lung carcinoma model in mice.

Although the exact mechanism by which the combination of CXCL10 with DDP can enhance the antitumor activity remained to be determined, the enhanced antitumor efficacy *in vivo* may in part result from the increased induction of the apoptosis in the combined treatment. This suggestion is supported by the present findings. The more apparent apoptotic cells in the tumors treated with CXCL10 + DDP

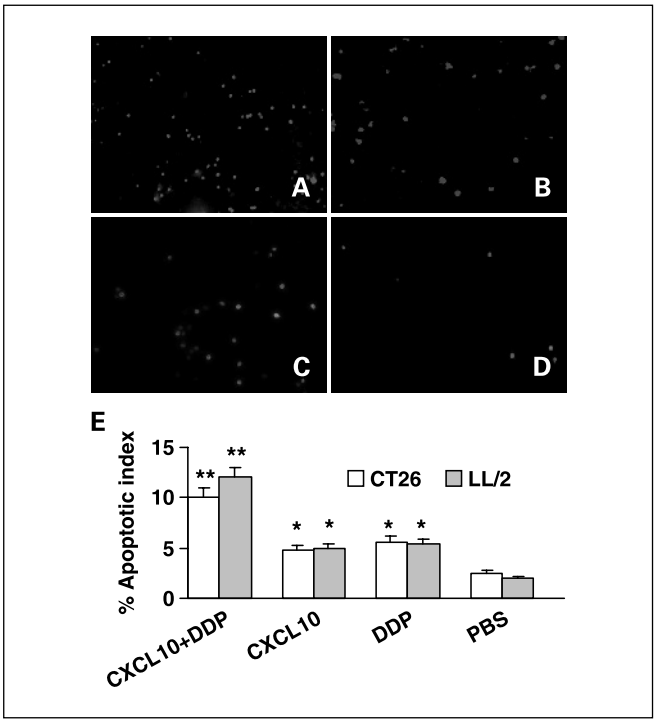

Fig. 5. Terminal deoxynucleotidyl transferase–mediated nick-end labeling staining of tumor tissues. Tumor tissue preparation and procedure for terminal deoxynucleotidyl transferase–mediated nick-end labeling staining were described in Materials and Methods. Representative sections from CT26 tumor tissue: CXCL10 + DDP (*A*), CXCL10 (*B*), DDP (*C*), and PBS (*D*). Apoptotic index within tissue from CT26 (*open columns*) and LL/2 (*solid columns*) from 10 mice (*E*). Sequential analysis showed systemic therapy with CXCL10 + DDP resulted in significant increment of apoptotic index versus PBS controls. (**, $P < 0.01$), CXCL10 or DDP alone versus PBS control (*, $P < 0.05$). *Columns*, mean apoptotic index of cancer cells; *bars*, ±SD.

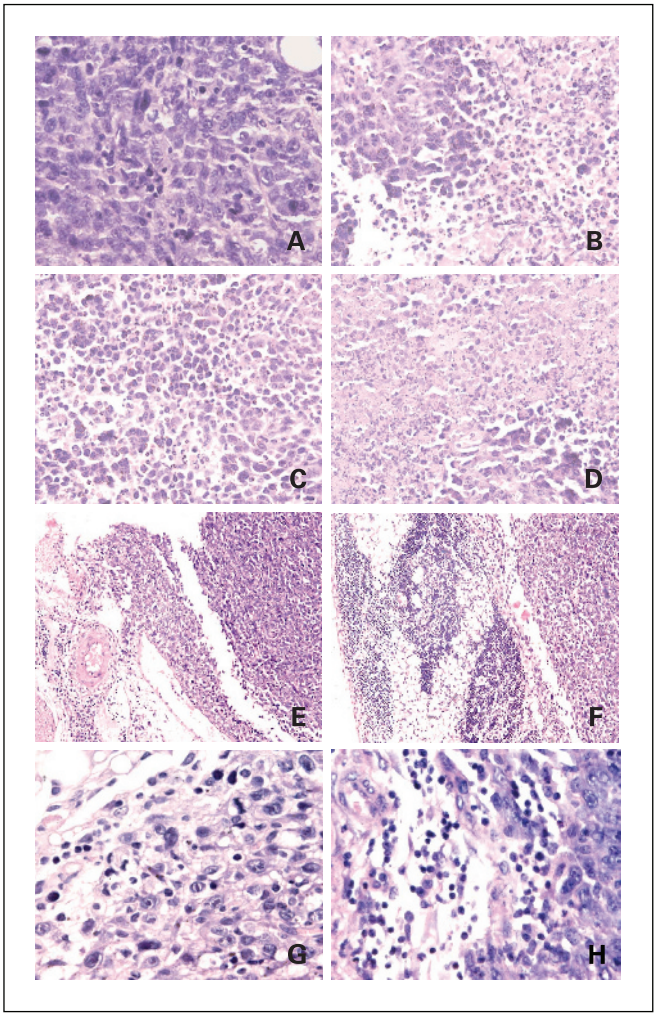

Fig. 6. Histochemical analysis of tumors. Tumor species were prepared as described in Materials and Methods. Sections of paraffin embedded from each group were stained with H&E. Tumor tissues from control mice had large areas of confluent tumor cells with little or no tumor tissue necrosis (*A*). Tumors with distinct necrosis were shown in DDP (*B*), CXCL10 (*C*), and DDP in conjunction with CXCL10 treated (*D*), respectively (×200). Leukocyte infiltration exhibiting clustering-like aggregation was apparently observed in the margin of CXCL10- or CXCL10 + DDP–treated group within CT26 and LL/2 tumor tissues. Little infiltration was found in the control of two models. Representative sections of PBS control (*E*) and CXCL10 (*F*) from CT26 neoplasm tissue were photomicrographed at ×100 magnification. In addition, lymphocyte infiltration was also enhanced in the central region of CXCL10- or CXCL10 + DDP–treated mice. Representative images of CT26 neoplasm tissue in PBS control (*G*) and CXCL10 (*H*) treated groups were depicted at ×400 magnification.

was found compared with the treatment with CXCL10 or DDP alone or no-treatment groups. DDP has been effective in inducing apoptosis in variety of tumor cell lines (40–42). Its apoptosis-inducing effects are known to be correlated with DNA damage by forming DNA-Pt adducts and DNA strand breaks (40, 41). Recently, evidence indicated that CXCL10 reduced microvessel density, leading to the observed increase in both tumor cell apoptosis and necrosis (43). Our findings that the induction of apoptosis and necrosis within tumor by the inhibition of angiogenesis with CXCL10 in our experiments are coincided with previous reports (22). Thus, we may speculate that the potent antiangiogenesis activity by CXCL10 may play an important role in retarding or preventing adequate nourishment of tumors during their regrowth after a chemotherapeutic insult, resulting in tumor growth stasis. The inhibition of angiogenesis by CXCL10, therefore, is complementary to antitumor treatments, as was seen in our experiments. The other agents, including soluble vascular endothelial growth factor receptor (44), angiostatin (45), endostatin (46, 47), etc., has been also reported to inhibit tumor angiogenesis, to induce apoptosis, and to suppress tumor growth. The molecular mechanisms underlying the inhibition of angiogenesis, which in turn result in the induction of apoptosis in tumor cells by these agents, have yet to be elucidated fully (48). Furthermore, the other findings have shown that the combination of an antiangiogenic agent such as TNP-470 (7), vascular endothelial growth factor receptor-2 antibody (49), squalamine (8, 50), etc., with chemotherapy can enhance tumor growth inhibition. Taken together, these findings mentioned above also support our suggestion that the enhanced antitumor efficacy in the present study may in part result from the increased induction of the apoptosis in the combined treatment. In addition, the penetration of anticancer agents to cells distant from the vascular system is required for efficacy of cancer chemotherapy against solid tumors (51, 52). Recently, evidences showed that IFN-γ could sensitize chemotherapy by promoting penetration of chemotherapeutic drugs into the tissue gap of the solid tumor (53). Therefore, we can not ignore the possibility that IP-10/CXCL10 improved the penetration of DDP into tumor tissues responsible for the enhanced antitumor activity and the increased induction of apoptosis. These proposed mechanisms are persuasive, but further experiments *in vitro* and *in vivo* will be necessary to resolve the relative contribution of the hypothesized mechanism.

It has been reported that the intratumor injection of CXCL10 proteins or CXCL10-transduced cells led to reduced tumor growth and the potent inhibition of angiogenesis in a mouse models of lung cancer or melanoma (22, 24). We also found that the intratumoral administration of CXCL10 have recruited apparent mononuclear cells and profoundly inhibited angiogenesis, compared with systemic administration of CXCL10 (data not shown). However, the rationale for administering CXCL10 systemically in the present study is based on our effort to imitate clinical practice of most recombinant protein given as systemical rather than intratumoral. In fact, it is difficult for a clinical doctor to administer recombinant CXCL10 intratumorally in case of human lung or colon carcinoma, unless the metastatic lesions are found near body surfaces. Thus, intratumoral administration of CXCL10 may have limited clinical application in the future. Our findings suggest that the administration of recombinant CXCL10 systemically is effective in the inhibition of tumor growth. One could also achieve better antitumor response by combining CXCL10 with other chemotherapies or radiation.

It had been speculated that IP-10/CXCL10 may afford hematologic chemoprotection (26, 27), in addition to its antitumor properties for the treatment of cancers. We determined cell cycles of hematopoietic in the marrow by flow cytometry. No statistically significant difference in percentages of G_0-G_1, S, and G_2-M phase distribution were found between CXCL10 at 10 and 25 μg per kg per day and PBS control, which indicated that CXCL10 was well tolerated at the present dose. Either accumulation of hematopoietic stem cells in the G_0 phase or reduction in the percentage of cells in the S phase was not observed. Therefore, unless protection was mediated by a transient growth suppression that had no effect on the number of colonies seen in present concurrent administration rather than sequential, cell cycle redistribution does not seem to explain myeloprotective effects of CXCL10 mediated through inhibition of primitive progenitors from entering cycling phase.

In summary, our data suggest that the combination of CXCL10, a well-tolerated angiogenesis inhibitor, with DDP can enhance the antitumor activity, and that the enhanced antitumor efficacy *in vivo* may in part result from the increased induction of the apoptosis in the combined treatment. The present findings may be of importance to the further exploration of the potential application of this combined approach in the treatment of lung and colon carcinoma.

References

1. The International Adjuvant Lung Cancer Trial Collaborative Group. Cisplatin-based adjuvant chemotherapy in patients with completely resected non-small-cell lung cancer. N Engl J Med 2004;350:351–60.
2. Folkman J. Seminars in medicine of the Beth Israel Hospital, Boston. Clinical applications of research on angiogenesis. N Engl J Med 1995;333:1757–63.
3. Marshall E. The road blocks to angiogenesis blockers. Science (Wash. DC) 1998;280:997–9.
4. Marx J. Angiogenesis: a boost for tumor starvation. Science (Wash. DC) 2003;301:452–4.
5. Garkavtsev I, Kozin SV, Chernova O, et al. The candidate tumor suppressor protein ING4 regulates brain tumor growth and angiogenesis. Nature 2004;428:328–32.
6. Teicher BA, Sotomayor EA, Huang ZD. Antiangiogenic agents potentiate cytotoxic cancer therapies against primary and metastatic disease. Cancer Res 1992;52:6702–4.
7. Kato T, Sato K, Kakinuma H, Matsuda Y. Enhanced suppression of tumor growth by combination of angiogenesis inhibitor *O*-(chloroacetyl-carbamoyl) fumagillol (TNP-470) and cytotoxic agents in mice. Cancer Res 1994;54:5143–7.
8. Schiller JH, Bittner G. Potentiation of platinum antitumor effects in human lung tumor xenografts by the angiogenesis inhibitor squalamine: effects on tumor neovascularization. Clin Cancer Res 1999;5:4287–94.
9. Strawn LM, Kabbinavar F, Schwartz DP, et al. Effects of SU101 in combination with cytotoxic agents on the growth of subcutaneous tumor xenografts. Clin Cancer Res 2000;6:2931–40.
10. Browder T, Butterfield CE, Kräling BM, et al. Antiangiogenic scheduling of chemotherapy improves efficacy against experimental drug-resistant cancer. Cancer Res 2000;60:1878–86.
11. Morioka H, Weissbach L, Vogel T, et al. Antiangiogenesis treatment combined with chemotherapy produces chondrosarcoma necrosis. Clin Cancer Res 2003;9:1211–7.
12. Strieter RM, Polverini PJ, Kunkel SL, et al. The functional role of the ELR motif in CXC chemokine-mediated angiogenesis. J Biol Chem 1995;270:27348–57.

13. Luster AD, Unkeless JC, Ravetch JV. γ-Interferon transcriptionally regulates an early-response gene containing homology to platelet proteins. Nature 1985;315:672–6.

14. Luster AD, Ravetch JV. Biochemical characterization of a γ interferon-inducible cytokine (IP-10). J Exp Med 1987;166:1084–97.

15. Ohmori Y, Hamilton TA. A macrophage LPS-inducible early gene encodes the murine homologue of IP-10. Biochem Biophys Res Commun 1990;168:1261–7.

16. Angiolillo AL, Sgadari C, Taub DD, et al. Human interferon-inducible protein 10 is a potent inhibitor of angiogenesis *in vivo*. J Exp Med 1995;182:155–62.

17. Romagnani P, Annunziato F, Lasagni L, et al. Cell cycle-dependent expression of CXC chemokine receptor 3 by endothelial cells mediates angiostatic activity. J Clin Invest 2001;107:53–63.

18. Luster AD, Leder P. CXCL10, a CXC chemokine, elicits a potent thymus-dependent antitumor response *in vivo*. J Exp Med 1993;178:1057–65.

19. Dufour JH, Dziejman M, Liu MT, Leung JH, Lane TE, Luster AD. IFN-γ-inducible protein 10 (IP-10; CXCL10)-deficient mice reveal a role for IP-10 in effector T cell generation and trafficking. J Immunol 2002; 168:3195–204.

20. Sgadari C, Angiolillo AL, Cherney BW, et al. Interferon-inducible protein-10 identified as a mediator of tumor necrosis *in vivo*. Proc Natl Acad Sci U S A 1996;93:13791–6.

21. Arenberg DA, Kunkel SL, Polverini PJ, et al. Interferon-γ-inducible protein (IP-10) is an angiostatic factor that inhibits human non-small cell lung cancer (NSCLC) tumorigenesis and spontaneous metastasis. J Exp Med 1996;184:981–92.

22. Arenberg DA, White ES, Burdick MD, Strom SR, Strieter RM. Improved survival in tumor-bearing SCID mice treated with interferon-γ-inducible protein 10 (IP-10/CXCL10). Cancer Immunol Immunother 2001;50:533–8.

23. Yao L, Pike SE, Pittaluga S, et al. Anti-tumor activities of the angiogenesis inhibitors interferon-inducible protein-10 and the calreticulin fragment vasostatin. Cancer Immunol Immunother 2002;51:358–66.

24. Feldman AL, Friedl J, Lans TE, et al. Retroviral gene transfer of interferon-inducible protein 10 inhibits growth of human melanoma xenografts. Int J Cancer 2002;99:149–53.

25. Mauceri HJ, Hanna NN, Beckett MA, et al. Combined effects of angiostatin and ionizing radiation in antitumour therapy. Nature 1998;394:287–91.

26. Han ZC, Lu M, Li JM, et al. Platelet factor 4 and other CXC chemokines support the survival of normal hematopoietic cells and reduce the chemosensitivity of cells to cytotoxic agents. Blood 1997;89:2328–35.

27. Sarris AH, Broxmeyer HE, Wirthmueller U, et al. Human interferon-inducible protein 10: expression and purification of recombinant protein demonstrate inhibition of early human hematopoietic progenitors. J Exp Med 1993;178:1127–32.

28. Towbin H, Staehelin T, Gordon J. Electrophoretic transfer of proteins from polyacrylamide gels to nitrocellulose sheets: procedure and some applications. Proc Natl Acad Sci U S A 1979;76:4350–4.

29. Taub DD, Lloyd AR, Conlon K, et al. Recombinant human interferon-inducible protein 10 is a chemoattractant for human monocytes and T lymphocytes and promotes T cell adhesion to endothelial cells. J Exp Med 1993;177:1809–14.

30. Liu JY, Wei YQ, Yang L, et al. Immunotherapy of tumors with vaccine based on quail homologous vascular endothelial growth factor receptor-2. Blood 2003;102:1815–23.

31. Hoffmann J, Schirner M, Menrad A, Schneider MR. A highly sensitive model for quantification of *in vivo* tumor angiogenesis induced by alginate-encapsulated tumor cells. Cancer Res 1997;57:3847–51.

32. He QM, Wei YQ, Tian L, et al. Inhibition of tumor growth with a vaccine based on xenogeneic homologous fibroblast growth factor receptor-1 in mice. J Biol Chem 2003;278:21831–6.

33. Vermeulen PB, Gasparini G, Fox SB, et al. Quantification of angiogenesis in solid human tumours: an international consensus on the methodology and criteria of evaluation. Eur J Cancer 1996;32:2474–84.

34. Wood JM, Bold G, Buchdunger E, et al. PTK787/ZK 222584, a novel and potent inhibitor of vascular endothelial growth factor receptor tyrosine kinases, impairs vascular endothelial growth factor induced responses and tumor growth after oral administration. Cancer Res 2000;60:2178–89.

35. Vindelov LL, Christensen IJ, Nissen NI. A detergent trypsin method for the preparation of nuclei for flow cytometric DNA analysis. Cytometry 1983;3:323–7.

36. Eton O, Talpaz M, Lee KH, Rothberg JM, Brell JM, Benjamin RS. Phase II trial of recombinant human interleukin-2 and interferon-α-2a: implications for the treatment of patients with metastatic melanoma. Cancer 1996;77:893–9.

37. Tulpule A, Joshi B, DeGuzman N, et al. Interleukin-4 in the treatment of AIDS-related Kaposi's sarcoma. Ann Oncol 1997;8:79–83.

38. Sparano JA, Gray R, Giantonio B, Dwyer PO, Comis RL. Evaluating antiangiogenesis agents in the clinic: the Eastern Cooperative Oncology Group portfolio of clinical trials. Clin Cancer Res 2004;10:1206–11.

39. Reimer CL, Agata N, Tammam JG, et al. Antineoplastic effects of chemotherapeutic agents are potentiated by NM-3, an inhibitor of angiogenesis. Cancer Res 2002;62:789–95.

40. Saris CP, van de Vaart PJ, Rietbroek RC, Blommaert FA. *In vitro* formation of DNA adducts by cisplatin, lobaplatin and oxaliplatin in calf thymus DNA in solution and in cultured human cells. Carcinogenesis 1996;17:2763–9.

41. Faivre S, Chan D, Salinas R, Woynarowska B, Woynarowski JM. DNA strand breaks and apoptosis induced by oxaliplatin in cancer cells. Biochem Pharmacol 2003;66:225–37.

42. Zhong X, Li X, Wang G, et al. Mechanisms underlying the synergistic effect of SU5416 and cisplatin on cytotoxicity in human ovarian tumor cells. Int J Oncol 2004;25:445–51.

43. Yang JM, Richmond A. The angiostatic activity of interferon-inducible protein-10/CXCL10 in human melanoma depends on binding to CXCR3 but not to glycosaminoglycan. Mol Ther 2004;9:846–55.

44. Takayama K, Ueno H, Nakanishi Y, et al. Suppression of tumor angiogenesis and growth by gene transfer of a soluble form of vascular endothelial growth factor receptor into a remote organ. Cancer Res 2000;60: 2169–77.

45. Yokoyama Y, Dhanabal M, Griffioen AW, Sukhatme VP, Ramakrishnan S. Synergy between angiostatin and endostatin: inhibition of ovarian cancer growth. Cancer Res 2000;60:2190–6.

46. Herbst RS, Mullani NA, Davis DW, et al. Development of biologic markers of response and assessment of antiangiogenic activity in a clinical trial of human recombinant endostatin. J Clin Oncol 2002;20:3804–14.

47. Schmidt NO, Ziu M, Carrabba G, et al. Antiangiogenic therapy by local intracerebral microinfusion improves treatment efficiency and survival in an orthotopic human glioblastoma model. Clin Cancer Res 2004;10:1255–62.

48. Folkman J. Angiogenesis and apoptosis. Semin Cancer Biol 2003;13:159–67.

49. Klement G, Baruchel S, Rak J, et al. Continuous low-dose therapy with vinblastine and VEGF receptor-2 antibody induces sustained tumor regression without overt toxicity. J Clin Invest 2000;105:15–24.

50. Williams J, Weitman S, Gonzalez CM, et al. Squalamine treatment of human tumors in *nu/nu* mice enhances platinum-based chemotherapies. Clin Cancer Res 2001;7:724–33.

51. Tunggal JK, Cowan DSM, Shaikh H, Tannock IF. Penetration of anticancer drugs through solid tissue: a factor that limits the effectiveness of chemotherapy for solid tumors. Clin Cancer Res 1999;5:1583–6.

52. Curnis F, Sacchi A, Corti A. Improving chemotherapeutic drug penetration in tumors by vascular targeting and barrier alteration. J Clin Invest 2002;110: 475–82.

53. Sacchi A, Gasparri A, Curnis F, Bellone M, Corti A. Crucial role for interferon γ in the synergism between tumor vasculature-targeted tumor necrosis factor α (NGR-TNF) and doxorubicin. Cancer Res 2004;64: 7150–5.